

Chiral symmetry and scale invariance breaking in spin chains

Cite as: AIP Advances **10**, 025215 (2020); <https://doi.org/10.1063/1.5130190>

Submitted: 24 October 2019 . Accepted: 28 November 2019 . Published Online: 11 February 2020

Felipe Torres, Miguel Kiwi, Nicolas M. Vargas, Carlos Monton, and Ivan K. Schuller

COLLECTIONS

Paper published as part of the special topic on [64th Annual Conference on Magnetism and Magnetic Materials](#)

Note: This paper was presented at the 64th Annual Conference on Magnetism and Magnetic Materials.



View Online



Export Citation



CrossMark

ARTICLES YOU MAY BE INTERESTED IN

[Comparing domain wall synapse with other non volatile memory devices for on-chip learning in analog hardware neural network](#)

AIP Advances **10**, 025111 (2020); <https://doi.org/10.1063/1.5128344>


[Interplay between doping and size effects on \$Y_{1-x}Eu_xMn_2O_5\$ nanorods](#)

AIP Advances **10**, 025017 (2020); <https://doi.org/10.1063/1.5129738>

[Dependence of the noise of an orthogonal fluxgate on the composition of its amorphous wire-core](#)

AIP Advances **10**, 025114 (2020); <https://doi.org/10.1063/1.5130393>



NEW



AVS Quantum Science

A new interdisciplinary home for impactful quantum science research and reviews

Co-Published by

NOW ONLINE



Chiral symmetry and scale invariance breaking in spin chains

Cite as: AIP Advances 10, 025215 (2020); doi: 10.1063/1.5130190
Presented: 7 November 2019 • Submitted: 24 October 2019 •
Accepted: 28 November 2019 • Published Online: 11 February 2020



Felipe Torres,¹ Miguel Kiwi,^{1,a)} Nicolas M. Vargas,² Carlos Monton,³ and Ivan K. Schuller²

AFFILIATIONS

¹Departamento de Física, Facultad de Ciencias, Universidad de Chile, Casilla 653, Santiago 7800024, Chile and Centro para el Desarrollo de la Nanociencia y la Nanotecnología, CEDENNA, Avda. Ecuador 3493, Santiago 9170124, Chile

²Department of Physics, University of California, San Diego, California 92093, USA

³General Atomics, P.O. Box 85608, San Diego, California 92186, USA

Note: This paper was presented at the 64th Annual Conference on Magnetism and Magnetic Materials.

a)Corresponding author: m.kiwi.t@gmail.com

ABSTRACT

The effects of the Dzyaloshinsky-Moriya interaction on finite size one-dimensional (1D) magnetic chains are investigated as a function of their length. The magnetic configuration the system adopts for varying boundary conditions are explored analytically, which leads to the appearance of chiral configurations that play a crucial role. The coercive and exchange bias fields show an unexpected chain length dependence, caused by the boundary conditions and by chiral symmetry breaking, which in turn leads to the breakdown of scale-invariance. Our treatment yields results in agreement with experimental evidence and ongoing research on phthalocyanine iron chains bonded to hydrogen.

© 2020 Author(s). All article content, except where otherwise noted, is licensed under a Creative Commons Attribution (CC BY) license (<http://creativecommons.org/licenses/by/4.0/>). <https://doi.org/10.1063/1.5130190>

As the size of a physical system reaches the nanometer scale the magnetic ordering energy decreases until it becomes comparable to thermal fluctuations, which destroy long-range correlations.¹ Here we examine sources of magnetic anisotropy induced by chiral symmetry breaking that quench fluctuations and which may stabilize low dimensional magnetic order, which was given theoretical justification² and achieved by several experimental groups.^{3–6} Indeed, the anomalous thermodynamic properties of quasi-one-dimensional molecular magnets,^{7–9} field-induced FM ordering,¹⁰ and the helical spin structure of Lanthanide chains¹¹ have been attributed to chiral magnetic states. In addition, Chen *et al.*¹² observed chirality-induced exchange-bias, which we obtain here theoretically. Moreover, Cinti *et al.*^{13,14} validated Villains conjecture,¹⁵ while Sessoli *et al.*¹⁶ observed strong magneto-chiral dichroism in a paramagnetic molecular helix.

In one-dimensional (1D) magnetic systems long-range ferromagnetic (FM) order can be achieved by the interaction between the magnetic atoms and their supporting frames, such as substrates or inert (non-magnetic) crystal lattices, in which the system is embedded. These interactions create magnetic anisotropy barriers that, in

combination with slow magnetic relaxation, may stabilize magnetic order.

While magnetic order in low dimensional systems has been a long time goal, achieving it has proved to be no easy task. On the one hand experiments are difficult to implement, and from a theoretical viewpoint the Mermin-Wagner theorem establishes a strong limitation: that there can be no spontaneous magnetic long-range order in one and two-dimensions at finite temperatures induced exclusively by short range magnetic interactions. However, experimental success was achieved some time ago,¹⁷ with the observation that monatomic chains of Co on a Pt substrate exhibit 1D local ferromagnetism. A theoretical understanding of the phenomenon was recently put forward,² on the basis of the addition to the exchange coupling of the Dzyaloshinsky-Moriya^{18–20} interaction, without any external magnetic anisotropy. It is relevant to point out that the fabrication of 1D physical systems with magnetic interactions are essential to address such relevant problems as quantum criticality,^{21–24} -body problems,^{23,25–27} spin transport,^{28–31} and new (topological) magnetic phases such as the ones predicted by Haldane.^{32,33}

We explore symmetry breaking as a consequence of size reduction, and the emergence of chiral symmetry as a stabilizing agent. The additional feature we include, and on which we focus our interest, is the Dzyaloshinsky-Moriya interaction (DMI). In particular, chiral magnetism in low-dimensional systems is caused by the spin-orbit interaction and inversion symmetry breaking, which in turn leads to the DMI.^{34,35} As already shown^{1,2,36-38} the superposition of short range direct exchange plus the DMI² stabilizes 1D and 2D magnetic order at low temperatures. In fact thermal and quantum fluctuations, that prevent the onset of long range order, compete against the spin correlations induced by short-range interactions, quenching order. However, spontaneous ordering arises once the short range DMI is incorporated. By reducing spin fluctuations the inclusion of the DMI generates a helical spin arrangement which turns out to be stable in one and two dimensions.²

The microscopic origin of the DMI is based on super-exchange theory including spin orbit coupling.¹⁸⁻²⁰ There are two different mechanisms that give rise to antisymmetric exchange between two metallic ions: the spin-orbit coupling between localized unpaired d-shell electrons in an inversion-asymmetric crystal field, and the indirect interaction of two magnetic ions through a non-magnetic one. Weak ferromagnetic order observed in the antiferromagnetic insulating compounds α -Fe₂O₃ and CrF₃ is attributed to the DMI,¹⁸⁻²⁰ as well as the low temperature phases of the perovskites³⁹⁻⁴¹ La₂CuO₄ and YBa₂Cu₃O₆.

A possible way to control chirality is by means of the boundary conditions a 1D chain is subject to. In fact, if the ends of the chain are subject to identical boundary conditions the magnetic symmetry will either be translationally invariant or at most will display some sort of helical order. However, if the chain ends are pinned in different directions a whole new spectrum of possible magnetic configurations becomes possible.

The energy of a FM spin chain, including the DMI, is given by

$$E_0 = - \sum_{i,j} [J \vec{s}_i \cdot \vec{s}_j + \vec{D}_{i,j} \cdot (\vec{s}_i \times \vec{s}_j)], \quad (1)$$

where J is the exchange coupling between neighboring atoms, $\vec{D}_{i,j}$ is the antisymmetric DM vector ($D_{i,j} = -D_{j,i}$). The chain is oriented along the z -direction, and its length is $\ell = Na$, where N is the total number of magnetic moments and a the lattice parameter. The DMI, which is induced by localized electrons, is oriented perpendicular to the z -axis. Locally, a parallel spin configuration is energetically preferred by the ferromagnetic exchange interaction, while a canted spin configuration is favored by this DMI. The competition between both interactions gives rise to two oppositely handed helical spin structures, where the handedness depends of the sign of DMI interaction. Using the DM vector as defined by Levy and Fert,⁴² we obtain $\vec{D}_{i,j} \sim \vec{r}_i \times \vec{r}_j$, where \vec{r}_i is the position of the i -th magnetic ion. In the vicinity of the chain ends the DMI produces an effective boundary anisotropy because of symmetry breaking. Indeed, if $\vec{D}_{N-1,N} \sim \vec{r}_{N-1} \times \vec{r}_N \sim D' \hat{x}$ then $\vec{D}_{1,2} \sim \vec{r}_1 \times \vec{r}_2 \sim -D' \hat{x}$. Therefore, at the chain ends the DMIs point in opposite directions, which means that the weak anisotropies are also aligned in opposite directions. Further, the boundary condition produces a left- and right-handed reverse mode. This chiral symmetry breaking creates two states with opposite chirality. The competition between them generates a local

anisotropy in the chain center, which depends on the length of the helical arrangement; hence, the magnetic reversal mode depends on the chain length.

In addition, since the magnetic moments lie in the x, y plane, we can specify the i -th magnetic spin as $\vec{s}_i = s[\cos(qai + \phi_i), c \sin(qai + \phi_i)]$, where \vec{q} is the spin wave-vector, and c is the chirality index $c = \{1, -1\}$ (right-handed, left-handed), and ϕ_i the initial phase. Using this parametrization Eq. (1) takes the form

$$E_0 = -s^2 \sum_{i,j} \left(J \cos[(i-j)qa + \Phi_{i,j}] - cD_{i,j} \sin[(i-j)qa + \Phi_{i,j}] \right), \quad (2)$$

with $\Phi_{i,j} = \phi_i - \phi_j$. Notice that the sign of the DMI is not uniquely determined. It is this feature the one that allows for an extra degree of freedom, and opens the possibility for the magnetic moments at the chain ends to align either parallel or forming a canting angle relative to each other; analytically, $\Phi_{1,N} = \phi_N - \phi_1$ can be equal to 0 (parallel) or $\Phi_{1,N} \neq 0$ (canted configuration), where 1 and N label the two end atoms of the linear chain.

We observe that the exchange interaction does not change with chirality; however, it appears explicitly in the DMI, which demonstrates that the DMI generates a chiral ground state.⁴³⁻⁴⁵ In the case of a spin chain the DM vector can be written as $D_{i,i+1} = (-1)^i D$, where the alternating sign $(-1)^i$ breaks the inversion symmetry with respect to the center between two neighbor FM ions.^{18-20,38} This way, using Eq. (1), we obtain

$$E_0 = -2s^2 \sum_i [J \cos(qa + \Phi_i) - (-1)^i cD \sin(qa + \Phi_i)]. \quad (3)$$

If $\Phi_i = \Phi$ for all i then $\sum_i (-1)^i \sin(qa + \Phi) = 0$, which means that DMI effects can be neglected; thus, the local phase is intimately related with the chirality. Indeed, boundary conditions play a significant role in the quenching of the chiral symmetry. Let us now include the fact that the end atoms of the chain are subject to anisotropy, so that Eq. (1) takes the form

$$E = E_0 + 2 \sum_i K(\hat{e}_i \cdot \vec{s}_i), \quad (4)$$

where \hat{e}_i is a unit vector in the x, y plane, and is differently oriented at the chain ends, but $\hat{e}_i = 0$ otherwise.

We now provide results derived using the scheme outlined above. We first study the dynamics of a 40 atom 1D FM chain with free end boundary conditions, as illustrated in the top left of Fig. 1, which gives rise to the hysteresis loop shown at its right. The hysteresis loops are obtained by minimization of the Eq. 4, and including a Zeeman interaction. The exchange bias field is defined as $H_{EB} = (H_R + H_L)/2$, and the coercive field as $H_C = (H_R - H_L)/2$, with $H_R(H_L)$ is the right (left) coercive field along the axis. When the chain end atoms are pinned parallel to each other, but forming an angle with the rest of the ferromagnetically aligned magnetic moments, as illustrated left middle of Fig. 1, exchange bias (H_{EB}) emerges as a consequence of the symmetry breaking imposed by the pinning, as shown to its right. However, the reversal mode for the above two cases corresponds to coherent rotation of the magnetic moments. Finally, we examine what happens for the canted configuration, defined by $\Phi_{1,N} \neq 0$, where 1 and N label the two pinned end

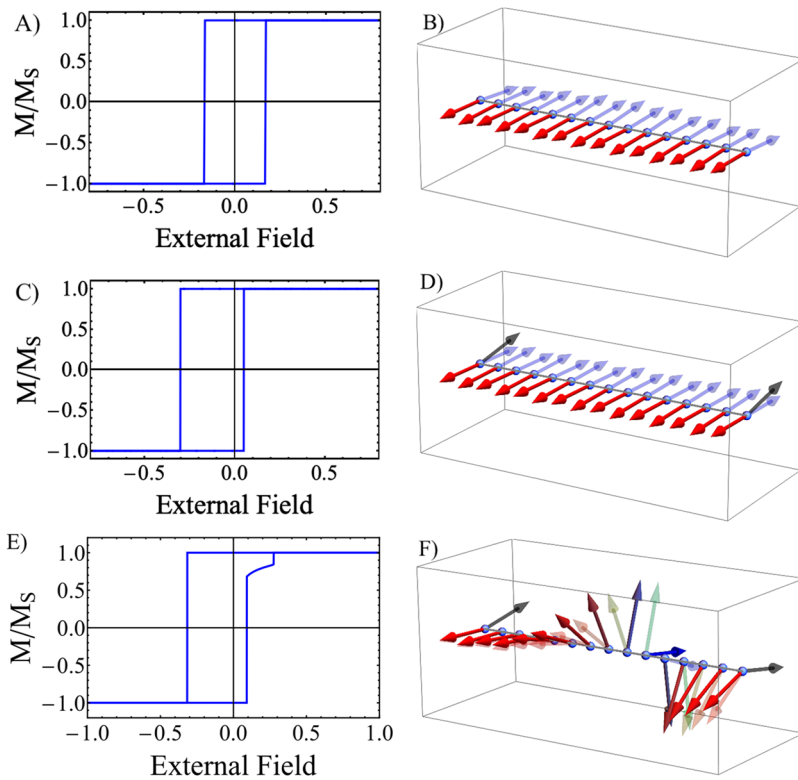


FIG. 1. Hysteresis loops for a 15 atom 1D chain and boundary-dependent magnetic spin chain configurations. A) Free end boundary conditions; C) end parallel spins pinned; and E) end spins canted. The corresponding sketch of the spin configurations are illustrated in B), D) and F), respectively. The negative exchange bias is due to the boundary anisotropy. The kink in the coercivity corresponds to the two step reversal mode predicted by Villain.¹⁵

atoms of the linear chain. In this case the complex chiral magnetic the structure bottom left of Fig. 1 results, accompanied as well by exchange bias, as seen to its right. The kink in the coercivity corresponds to the two step reversal mode predicted by Villain.¹⁵ Thus, we notice that the various boundary conditions the chain ends are subject to significantly modify the magnetic configuration and the consequent exchange bias field H_{EB} .

Due to long-range spin correlations the chiral magnetic order ground state is characterized by a long-wavelength helical modulation. When the size of the system is less than this wavelength magnetic order is destroyed. We show that due to chiral symmetry breaking as the size of the chain increases the coercive field and the the exchange bias field reach saturation values, which implies scale invariance breakdown.

Scale invariant quantities correspond to homogeneous functions, satisfying the rescaling symmetry condition

$$H(\lambda\ell) = \lambda^\eta H(\ell). \quad (5)$$

As shown in Fig. 2 the coercive field for free boundary condition chains decays as $H_C \sim 1/\ell^\eta$, with $\eta \sim 4/5$ and there is no H_{EB} . Thus, scale invariance is preserved, even though the DMI has been included. The boundary condition effects on the exchange bias field H_{EB} and the coercive field H_C are illustrated in Fig. 3.

It is apparent that, after the absolute value of the magnitude of the exchange bias ($H_{EB} < 0$) goes through a maximum, there is a competition between the chiral configuration and the pinning at the chain ends. In Fig. 3 we show the unexpected length dependence of

the exchange bias H_{EB} and the coercive H_C fields as a function of chain length, for canted boundary conditions (a similar behavior is displayed for parallel pinned boundary conditions). We notice that after an initial increase the coercivity becomes length independent for large chains ($N \rightarrow \infty$). The relevance of the chiral kink in Fig. 3 disappears as the chain becomes large enough. From numerical calculation we obtain the H_{EB} and H_C profile, as shown in Fig. 3, which are used to fit the length-dependence of this fields, and are given by

$$H_{EB} = -1 + \alpha_{EB} e^{-\ell/\ell_0}, \quad (6)$$

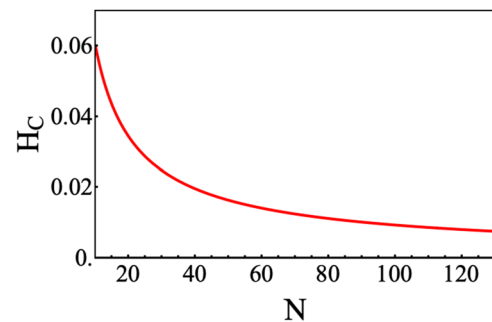


FIG. 2. Length-dependence of the coercive field. Decay of the coercive field for a free boundary condition chain. In this case there is no exchange-bias field.

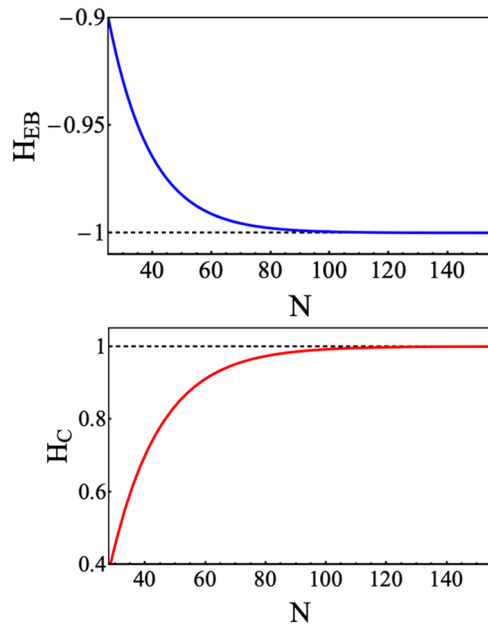


FIG. 3. (Upper panel) Exchange bias (H_{EB}) vs. chain length. (Lower panel) Coercive field H_C vs. chain length for the boundary conditions depicted in Fig. 1f. The field strengths are normalized to their saturation values.

$$H_C = 1 - \alpha_c e^{-\ell/\ell_0}, \quad (7)$$

where $\ell_0 \sim 15a$, $\alpha_{EB} = 0.6$, and $\alpha_c = 3.4$. Clearly the exponential factor breaks the scale-invariance. This symmetry breaking is attributed to the mismatch between the chiral magnetic order wavelength ℓ_0 and the chain length ℓ . When the wavelength of the chiral state is larger than the system size in which is embedded, *i.e.* when $\ell \rightarrow 0$, or when the length of the chain $\ell \gg \ell_0$, then the effects of the DMI vanish and scale-invariance is restored (see Eq. 7). For intermediate sizes H_{EB} and H_C are related through

$$H_{EB} - 1 = \frac{\alpha_{EB}}{\alpha_c} (1 - H_C). \quad (8)$$

The above equation shows a linear relation between the H_{EB} and H_C fields, caused by the propagation of chiral spin waves that originate on opposite ends of the chain. While the physical mechanism that gives rise to exchange bias is the interface exchange interaction between two materials with different magnetic properties, the coercivity depends on global magnetic anisotropies, such as magneto-crystalline or shape anisotropy. However, in our case these fields are intimately related and both arise from the same physical mechanism. Notice that there are no global sources of magnetic anisotropy in our model, thus only short-range interactions and symmetry breaking give rise to magnetic order. Therefore, the chiral reversal mode asymmetry yields simultaneously the nonzero H_{EB} and H_C fields. In addition, from Eq. 5 we also obtain an expression for the ratio of the H_R and H_L coercive fields

$$\frac{H_R}{2 - H_L} = \frac{\alpha_c - \alpha_{EB}}{\alpha_c + \alpha_{EB}}, \quad (9)$$

which means that when $H_{EB} = 0$

$$H_C = \frac{2\mu}{1 + \mu}, \quad (10)$$

where $\mu = (\alpha_c - \alpha_{EB})/(\alpha_c + \alpha_{EB})$. This expression differs from exponential decay for free boundary conditions.

In conclusion, we have put forward a model for magnetic linear chains subject to a variety of boundary conditions, and including the Dzyaloshinsky-Moriya interaction, in agreement with experimental evidence for chiral magnetic states in 1D. The model yields a length dependent coercivity which is in agreement with numerical simulation. The experimental verification of our results requires manipulation of small nanostructured, quasi 1D systems, with controlled boundary conditions. Recently 1D phthalocyanine iron (FePc) chains embedded into FePc/metal-free phthalocyanine (H_2Pc) superlattices have been fabricated using organic molecular beam epitaxy, and which allows for control of boundary conditions and chain length. Low temperature magnetic characterization reveals a length-dependence of the coercive field in SL arrays, while the coercive field for free boundary conditions chain remains almost constant.^{12,13,15,16,46} Our findings put forward a new strategy to study magnetic properties of spin chains with chiral symmetry breaking.

This is a highly interactive work. The ideas were motivated and discussed among the authors, the manuscript and its multiple version and the contributions of UCSD authors were supported by the U.S. Department of Energy Office of Basic Energy Science, DMR under grant DE FG02 87ER-45332. F. Torres, and M. Kiwi acknowledge financial support from grants FA9550-16-1-0122, FA9550-18-1-0438, Fondecyt 1160639, and CEDENNA through the Financiamiento Basal para Centros Científicos y Tecnológicos de Excelencia-FB0807. Supported by the U.S. Department of Energy AFOSR Office of Basic Energy Science.

REFERENCES

- N. D. Mermin and H. Wagner, *Phys. Rev. Lett.* **17**, 1133 (1966).
- F. Torres, D. Altbir, and M. Kiwi, *Eur. Phys. Lett.* **106**, 47004 (2014).
- R. Clérac, H. Miyasaka, M. Yamashita, and C. Coulon, *J. Am. Chem. Soc.* **124**, 12837 (2002).
- V. Skumryev, S. Stoyanov, Y. Zhang, G. Hadjipanayis, D. Givord, and J. Nogués, *Nature* **423**, 850 (2003).
- J. Eisenmenger and I. K. Schuller, *Nature Materials* **2**, 437 (2003).
- D. Visinescu, A. M. Madalan, M. Andruh, C. Duhayon, J.-P. Sutter, L. Ungur, W. Van den Heuvel, and L. F. Chiboratu, *Chemistry—A European Journal* **15** (2009).
- F. Bartolomé, J. Bartolomé, C. Benelli, A. Caneschi, D. Gatteschi, C. Paulsen, M. Pini, A. Rettori, R. Sessoli, and Y. Volokitin, *Phys. Rev. Lett.* **77**, 382 (1996).
- A. Lascialfari, R. Ullu, M. Affronte, F. Cinti, A. Caneschi, D. Gatteschi, D. Rovai, M. Pini, and A. Rettori, *Phys. Rev. B* **67**, 224408 (2003).
- A. Lascialfari, R. Ullu, M. Affronte, F. Cinti, A. Caneschi, D. Gatteschi, D. Rovai, M. Pini, and A. Rettori, *J. Magn. Magn. Mater.* **272-276**, 1052 (2004).
- B. K. Shaw, M. Das, A. Bhattacharyya, B. N. Ghosh, S. Roy, P. Mandal, K. Rissanen, S. Chattopadhyay, and S. K. Saha, *RSC Adv.* **6**, 22980 (2016).
- I. Mihalcea, M. Perfetti, F. Pineider, L. Tesi, V. Mereacre, F. Wilhelm, A. Rogalev, C. E. Anson, A. K. Powell, and R. Sessoli, *Inorganic Chemistry* **55**, 10068 (2016).
- K. Chen, A. Philippi-Kobs, V. Lauter, A. Vorobiev, E. Dyadkina, V. Yakovchuk, S. Stolyar, and D. Lott, *Phys. Rev. Applied* **12**, 024047 (2019).

- ¹³F. Cinti, A. Rettori, M. Pini, M. Mariani, E. Micotti, A. Lascialfari, N. Papinutto, A. Amato, A. Caneschi, D. Gatteschi, and M. Affronte, *Journal of Magnetism and Magnetic Materials* **322**, 1259 (2010).
- ¹⁴F. Cinti, A. Rettori, M. Pini, M. Mariani, E. Micotti, A. Lascialfari, N. Papinutto, A. Amato, A. Caneschi, D. Gatteschi, and M. Affronte, *Phys. Rev. Lett.* **100**, 057203 (2008).
- ¹⁵J. Villain, *J. Phys. C: Solid State Phys.* **10**, 4793 (1977).
- ¹⁶R. Sessoli, M.-E. Boulon, A. Caneschi, M. Mannini, L. Poggini, Fabrice Wilhelm, and A. Rogalev, *Nature Phys.* **11**, 69 (2015).
- ¹⁷J. Eisenmenger and I. K. Schuller, *Nat. Mat.* **2**, 437 (2003).
- ¹⁸I. Dzyaloshinsky, *J. Phys. Chem. Solids* **4**, 241 (1999).
- ¹⁹T. Moriya, *Phys. Rev. Lett.* **4**, 228 (1960).
- ²⁰T. Moriya, *Phys. Rev.* **120**, 91 (1960).
- ²¹B. C. Watson, V. N. Kotov, M. W. Meisel, D. W. Hall, G. E. Granroth, W. T. Montfrooij, S. E. Nagler, D. A. Jensen, R. Backov, M. A. Petruska, G. E. Fanucci, and D. R. Talham, *Phys. Rev. Lett.* **86**, 5168 (2001).
- ²²S. Sachdev, *Science* **288**, 475 (2000).
- ²³B. Lake, D. A. Tennant, C. D. Frost, and S. E. Nagler, *Nature Materials* **4**, 329 (2005).
- ²⁴R. Coldea, D. A. Tennant, E. M. Wheeler, E. Wawrzynska, D. Prabhakaran, M. Telling, K. Habicht, P. Smeibidl, and K. Kiefer, *Science* **327**, 177 (2010).
- ²⁵C. N. Yang, *Phys. Rev. Lett.* **19**, 1312 (1967).
- ²⁶H. L. Haselgrove, M. A. Nielsen, and T. J. Osborne, *Phys. Rev. A* **69**, 032303 (2004).
- ²⁷M. Girardeau, *J. Math. Phys.* **1**, 516 (1960).
- ²⁸Z. Zanolli, G. Onida, and J. C. Charlier, *ACS Nano* **4**, 5174 (2010).
- ²⁹C. Ramanathan, P. Cappellaro, L. Viola, and D. G. Cory, *New J. Phys.* **13**, 103015 (2011).
- ³⁰T. J. Osborne and N. Linden, *Phys. Rev. A* **69**, 052315 (2004).
- ³¹E. Coronado and M. Yamashita, *Dalton Trans.* **45**, 16553 (2016).
- ³²F. D. M. Haldane, *Phys. Lett.* **93A**, 464 (1983).
- ³³F. D. M. Haldane, *Phys. Rev. Lett.* **50**, 1153 (1983).
- ³⁴A. Kubetzka, M. Bode, O. Pietzsch, and R. Wiesendanger, *Phys. Rev. Lett.* **88**, 057201 (2002).
- ³⁵M. Heide, G. Bihlmayer, and S. Blügel, *Phys. Rev. B* **78**, 140403 (2008).
- ³⁶N. D. Mermin, *Phys. Rev.* **176**, 250 (1968).
- ³⁷S. A. Zvyagin, *Low Temp. Phys.* **38**, 819 (2012).
- ³⁸I. Affleck and M. Oshikawa, *Phys. Rev. B* **60**, 1038 (1999).
- ³⁹T. Thio, T. R. Thurston, N. W. Preyer, P. J. Picone, M. A. Kastner, H. P. Jenssen, D. R. Gabbe, C. Y. Chen, R. J. Birgeneau, and A. Aharony, *Phys. Rev. B* **38**, 905 (1988).
- ⁴⁰D. Coffey, T. M. Rice, and F. C. Zhang, *Phys. Rev. B* **44**, 10112 (1991).
- ⁴¹L. Shekhtman, O. Entin-Wohlman, and A. Aharony, *Phys. Rev. Lett.* **69**, 836 (1992).
- ⁴²P. Levy and A. Fert, *Phys. Rev. B* **23**, 4667 (1981).
- ⁴³I. A. Sergienko and E. Dagotto, *Phys. Rev. B* **73**, 094434 (2006).
- ⁴⁴K. Zakeri, Y. Zhang, J. Prokop, T.-H. Chuang, N. Sakr, W. X. Tang, and J. Kirschner, *Phys. Rev. Lett.* **104**, 137203 (2010).
- ⁴⁵L. Udvardi and L. Szunyogh, *Phys. Rev. Lett.* **102**, 207204 (2009).
- ⁴⁶N. M. Vargas, I. K. Schuller, and C. Monton, private communication (2019).